

The dopamine receptor D₅ gene shows signs of independent erosion in toothed and baleen whales

Luís Q. Alves^{1,2}, Juliana Alves^{1,2}, Rodrigo Ribeiro^{1,2}, Raquel Ruivo^{Corresp.,1}, Filipe Castro^{Corresp.,1}

¹ CIIMAR-University of Porto, Matosinhos, Portugal

² FCUP- University of Porto, Porto, Portugal

Corresponding Authors: Raquel Ruivo, Filipe Castro
Email address: rruivo@ciimar.up.pt, filipe.castro@ciimar.up.pt

To compare gene *loci* considering a phylogenetic framework is a promising approach to uncover the genetic basis of human diseases. Imbalance of dopaminergic systems is suspected to underlie some emerging neurological disorders. The physiological functions of dopamine are transduced via G-protein-coupled receptors, including DRD₅ which displays a relatively higher affinity towards dopamine. Importantly, DRD₅ knockout mice are hypertense, a condition emerging from an increase in sympathetic tone. We investigated the evolution of DRD₅, a high affinity receptor for dopamine, in mammals. Surprisingly, among 124 investigated mammalian genomes, we found that Cetacea lineages (Mysticeti and Odontoceti) have independently lost this gene, as well as the burrowing *Chrysochloris asiatica* (Cape golden mole). We suggest that DRD₅ inactivation parallels hypoxia-induced adaptations, such as peripheral vasoconstriction required for deep-diving in Cetacea, in accordance with the convergent evolution of vasoconstrictor genes in hypoxia-exposed animals. Our findings indicate that Cetacea are natural knockouts for DRD₅ and might offer valuable insights into the mechanisms of some forms of vasoconstriction responses and hypertension in humans.

1 The dopamine receptor D_5 gene shows signs of independent 2 erosion in Toothed and Baleen whales

3

4 Luís Q. Alves^{1,2}, Juliana Alves^{1,2}, Rodrigo Ribeiro^{1,2}, Raquel Ruivo¹, L. Filipe C. Castro^{1,2}

5

6 ¹ CIIMAR-University of Porto, Matosinhos, Portugal7 ² FCUP-University of Porto, Porto, Portugal

8

9 Corresponding Authors:

10 Filipe Castro and Raquel Ruivo

11 Avenida General Norton de Matos, S/N, Matosinhos, 4450-208, Matosinhos, Portugal

12 Email address: ruiivo@ciimar.up.pt; filipe.castro@ciimar.up.pt

13

14 Abstract

15 To compare gene *loci* considering a phylogenetic framework is a promising approach to uncover the
16 genetic basis of human diseases. Imbalance of dopaminergic systems is suspected to underlie some
17 emerging neurological disorders. The physiological functions of dopamine are transduced via G-protein-
18 coupled receptors, including DRD_5 which displays a relatively higher affinity towards dopamine.

19 Importantly, DRD_5 knockout mice are hypertense, a condition emerging from an increase in sympathetic
20 tone. We investigated the evolution of DRD_5 , a high affinity receptor for dopamine, in mammals.

21 Surprisingly, among 124 investigated mammalian genomes, we found that Cetacea lineages (Mysticeti
22 and Odontoceti) have independently lost this gene, as well as the burrowing *Chrysochloris asiatica* (Cape
23 golden mole). We suggest that DRD_5 inactivation parallels hypoxia-induced adaptations, such as
24 peripheral vasoconstriction required for deep-diving in Cetacea, in accordance with the convergent
25 evolution of vasoconstrictor genes in hypoxia-exposed animals. Our findings indicate that Cetacea are
26 natural knockouts for DRD_5 and might offer valuable insights into the mechanisms of some forms of
27 vasoconstriction responses and hypertension in humans.

28

29

30

31

32

33

34

35

36

37

38

39

40 Introduction

41 Dopamine is a neurotransmitter essential for brain function, regulating various physiological
42 processes including locomotion, cognition, and neuroendocrine functions (Hollon et al., 2002;
43 Ott & Nieder, 2018). Dopamine molecular actions are transduced *via* a specific group of G-
44 protein coupled receptors entailing two major classes: DRD₁-like and DRD₂-like receptors
45 (Beaulieu & Gainetdinov, 2011; Opazo et al., 2018). While DRD₁-like receptors stimulate cAMP
46 production postsynaptically, DRD₂-like receptors inhibit cAMP production both pre and
47 postsynaptically (Beaulieu & Gainetdinov, 2011). The genomic structure of the underlying genes
48 is also distinct, with DRD₁-like receptors yielding single exon coding regions (Beaulieu &
49 Gainetdinov, 2011). DRD₁₋₂ receptor classes have diversified in vertebrate evolution most likely
50 as a result of genome duplications (Opazo et al., 2018). Interestingly, agonist and antagonist
51 amino acid site conservation suggests evolutionary stasis of dopaminergic pathways (Opazo et
52 al., 2018). Among DRD₁-like receptors, the DRD₅ subtype displays distinctive features, namely
53 a relatively higher affinity towards dopamine, a putative agonist-independent activity and low
54 level, yet widespread, brain expression (Beaulieu & Gainetdinov, 2011; Ciliax et al., 2000;
55 Sunahara et al., 1991; Tiberi & Caron, 1994). Nonetheless, the DRD₅ seems to display distinct
56 regional and cellular distribution patterns in the brain, when compared to the DRD₁ and DRD₂
57 subtypes, with protein enrichment detected in the cerebral cortex, hippocampus and basal ganglia
58 (Ariano et al., 1997; Ciliax et al., 2000). Peripheral expression has also been found in the
59 adrenals (Dahmer & Senogles, 1996), kidney (Sanada et al., 2000) and gastrointestinal tract
60 (Mezey et al., 1996). Despite the association with schizophrenia (Muir et al., 2001), attention-
61 deficit/hyperactive disorder (Daly et al., 1999) and substance abuse (Vanyukov et al., 1998),
62 gene targeting studies revealed that DRD₅ knock-out mice develop hypertension, showing
63 increased blood pressure from 3 months of age (Hollon et al., 2002). This hypertensive
64 phenotype appears to result from a central nervous system defect, leading to an increase in
65 sympathetic tone and, consequently, vasoconstriction (Hollon et al., 2002). Besides neuronal
66 impairment, DRD₅ disruption was also suggested to increase the expression of the
67 prohypertensive Angiotensin II Type 1 Receptor (AT₁R), involved in renal salt balance, blood
68 pressure and vasoconstriction (Li et al., 2008). In fact, renal dopamine was suggested to promote
69 salt excretion, counter-regulating AT₁R and lowering hypertensive states (Hong et al., 2017; Li
70 et al., 2008; Zeng et al., 2005).

71 Whole genome sequencing has greatly expanded our capacity to comprehend evolutionary
72 history, the role of adaptation or the basis for phenotype differences across the tree of life. Multi-
73 genome comparisons have also been powerful to recognize the molecular basis of human
74 diseases, a field named as phylomedicine (Emerling et al., 2017; Kumar et al., 2011; Miller &
75 Kumar, 2001; Springer & Murphy, 2007). Here we investigate the evolution of DRD₅ in
76 mammalian species. By analyzing 124 genomes covering 16 orders, we show that independent
77 coding-debilitating mutations occurred in the ancestors of Mysticeti, of *Physeter catodon* (sperm
78 whale) and the remaining Odontoceti, strongly suggesting that DRD₅ is non-coding in Cetacea.
79 Reductive episodes have been widely documented across the tree of life contributing to
80 organismal divergence and physiological and morphological adaptation to environmental cues
81 (Albalat & Canestro, 2016; Braun, 2003; Jeffery, 2009; Olson, 1999). In agreement, gene loss
82 mechanisms seem pervasive in lineages that endured drastic habitat transitions in the course of
83 evolution, such as Cetacea, entailing niche-specific adaptations (Huelsmann et al., 2019; Lachner
84 et al., 2017; Lopes-Marques et al., 2019b; McGowen et al., 2014; Nery et al., 2014; Sharma et
85 al., 2018; Strasser et al., 2015). Thus, our findings suggest that these species are natural KOs for
86 this dopamine receptor and might offer valuable insights into the mechanisms of some forms of
87 essential hypertension.

88

89 **Materials & Methods**

90

91 To manually infer the coding status of DRD₅ genes, the following strategy was used:
92 first, gene orthology was assessed *via* synteny analysis, to clarify cases where gene annotation
93 was not found, as well as to define genomic regions to be posteriorly collected for gene
94 annotation (see supplementary figure 1). Next, open reading frame (ORF) manual annotation was
95 performed to detect eventual ORF-abolishing mutations. At least one mutation being posteriorly
96 validated using unassembled genomic sequencing reads available at the NCBI (National Center
97 of Biotechnology Information) Sequence Read Archive (SRA) database. Finally, dN/dS analyses
98 were also conducted to further investigate the inactive status of DRD₅ in Cetacea (see below).

99

100 **Synteny analysis**

101 To build the synteny maps for the DRD₅ gene *locus* in Cetacea and *Hippopotamus*
102 *amphibius* (hippopotamus) several annotated Cetacea genome assemblies were inspected and

103 scrutinised using the NCBI browser, namely *Orcinus orca* (killer whale; GCF_000331955.2),
104 *Lagenorhynchus obliquidens* (Pacific white-sided dolphin; GCF_003676395.1), *Tursiops*
105 *truncatus* (common bottlenose dolphin; GCF_001922835.1), *Delphinapterus leucas* (beluga
106 whale; GCF_002288925.1), *Neophocaena asiaeorientalis asiaeorientalis* (Yangtze finless
107 porpoise; GCF_003031525.1), *Lipotes vexillifer* (Yangtze River dolphin; GCF_000442215.1),
108 *Physeter catodon* (sperm whale; GCF_002837175.1) and *Balaenoptera acutorostrata scammoni*
109 (minke whale; GCF_000493695.1). *Bos taurus* (cattle; GCF_002263795.1), a fully terrestrial
110 relative of extant cetaceans, was used as reference. Next, (1) in genome assemblies with
111 annotated DRD₅, the following procedure was used: five protein-coding genes, upstream and
112 downstream of the DRD₅ gene, and from the same strand, were collected; (2) if DRD₅ gene
113 annotations were not present, the genomic *locus* was retrieved using *Bos taurus* (cattle) DRD₅
114 flanking genes as reference. The selected anchoring genes to search upstream and downstream
115 DRD₅ neighbouring genes were CPEB2 and OTOP1, respectively. Regarding *Hippopotamus*
116 *amphibius* (hippopotamus), the synteny map was built via blast searches against the assembled,
117 fragmented and not annotated genome of the same species, available at NCBI
118 (GCA_002995585.1). *Bos taurus* (cattle) DRD₅ flanking genes were used as reference; using the
119 discontinuous megablast task from blastn, the best blast hit (highest alignment identity and query
120 coverage) was retrieved and the coordinates of the alignment in the target genome carefully
121 inspected. The *Hippopotamus amphibius* (hippopotamus) synteny map was then built by sorting
122 the genes according to the subject alignment coordinates within genes, aligning at the same
123 genomic scaffold.

124

125 **Sequence retrieval and gene annotation**

126 The NCBI ‘low-quality protein’ (LQ) tag marks RefSeq sequences that have been modified
127 in order to correct open reading frame (ORF) indels present in the source genomic sequence,
128 which may arise from genome assembly errors; or, in some cases correspond to real sequence
129 modifications leading to shifts in the predicted ORF, resulting in non-conserved, or even
130 nonsense codons. For this reason, to clarify the functional status of DRD₅ in species presenting
131 LQ tag for this gene, the corresponding genomic regions were directly collected from NCBI.

132 Concerning species with no annotated DRD₅ genes two scenarios were identified: (1)
133 annotated genomes excluding DRD₅ gene annotation and (2) un-annotated genomes. Regarding

134 the first case (i.e. the cetaceans *Lipotes vexillifer*, the Yangtze River dolphin and *Balaenoptera*
135 *acutorostrata scammoni*, the minke whale, as well as other non-cetacean mammals), the DRD₅
136 genomic *locus* was retrieved using, as reference, annotated DRD₅ flanking genes, from
137 phylogenetically related species (*Bos taurus* (cattle) for cetaceans, regarding non-cetacean
138 mammals see Supplementary Table 1). If the genomic *locus* exhibited severe genomic
139 fragmentation (presence of Ns), hindering the retrieval using neighbouring genes, blastn searches
140 were conducted against the Whole Shotgun Contigs dataset of the corresponding species *via*
141 discontinuous megablast task, using as query the DRD₅ coding sequence of the same reference
142 species (Supplementary Table 1). The genomic sequence corresponding to the blast hit with the
143 highest alignment identity and query coverage was selected.

144 For species with no annotated genomes (i.e. *Balaenoptera bonaerensis* (Antarctic minke
145 whale), *Eschrichtius robustus* (grey whale), *Balaena mysticetus* (bowhead whale), *Sousa*
146 *chinensis* (Indo-pacific humpbacked dolphin), as well as *Hippopotamus amphibius*
147 (hippopotamus)) genomic sequences were retrieved through blastn searches in the corresponding
148 genome assembly using the *Bos taurus* (cattle) DRD₅ coding sequence as query. For each
149 species, the best genomic scaffold corresponded to the blast hit with the highest query coverage
150 and identity value. Due to the presence of a fragmented genomic region in the DRD₅ gene
151 annotation of *T. truncatus* (common bottlenose dolphin), the same blast search procedure was
152 carried out for this species, using as target the Whole Genome Shotgun contig dataset of the
153 same species; subsequent gene annotation was performed in the retrieved genomic contig.

154 Collected genomic sequences were further imported into Geneious Prime 2019
155 (www.geneious.com) and the DRD₅ gene coding sequences manually annotated for each species.
156 Briefly, using the built-in map to reference tool with the highest sensibility parameter selected,
157 the reference single-exon DRD₅ gene, 3' and 5' UTR flanked, was mapped against the
158 corresponding genomic sequence of the in-study species and aligned regions carefully screened
159 for ORF abolishing mutations including frameshift mutations and in-frame premature stop
160 codons. For Cetacea and *Hippopotamus amphibius* (hippopotamus) DRD₅ gene annotation, *Bos*
161 *taurus* (cattle) DRD₅ was selected as reference. Regarding non-cetacean mammals DRD₅
162 annotation, different references were chosen according to the phylogenetic relationships between
163 reference and test species (Supplementary Table 1). Finally, the identified mutations were next
164 validated using unassembled sequencing reads retrieved from at least two independent genomic

165 NCBI sequence read archive (SRA) projects (when available). Briefly, blastn searches were
166 conducted against the selected SRA projects (Supplementary Materials 1, 2 and 3) using as query
167 the nucleotide sequence containing the mutation. Blast hits were imported into Geneious Prime
168 2019 and mapped against the manually annotated sequences, using the built-in map to reference
169 tool, to confirm the presence of the identified mutation.

170

171 **Phylogenetic and dN/dS analyses**

172 The predicted cetacean and *Hippopotamus amphibius* (hippopotamus), DRD₅ coding
173 sequences, as well as the DRD₅ coding sequences of *Homo sapiens* (human) and *Bos taurus*
174 (cattle) available at NCBI were translation aligned in Geneious Prime 2019 using the Blosum62
175 substitution matrix. The alignment (1440 bp) was manually inspected and predicted DRD₅
176 coding sequences involved in alignment suffered prior inspection, with frameshift insertions and
177 deletions being omitted and stop codons recorded as missing. The alignment was posteriorly
178 exported for phylogenetic analysis. A Maximum likelihood phylogenetic tree, performed in
179 PhyML3.0 server (Guindon et al., 2010), was produced with the best sequence evolutionary
180 model being determined using the built-in smart model selection (HKY85 +G) (Lefort et al.,
181 2017). Node support was inferred based on 100 bootstrap replicates. The resulting phylogenetic
182 tree newick file is available as supplementary data (Supplementary File 1) and was subsequently
183 imported for visualisation in FigTree (Supplementary Material 4) (Rambaut & Drummond,
184 2012).

185 PAML 4.6 (Yang, 2007) was used to estimate the ratio (ω) of the nonsynonymous
186 substitution rate (dN) to the synonymous substitution rate (dS) using the produced phylogenetic
187 tree (Supplementary Material 4). Codeml with the branch model was implemented to estimate
188 dN/dS ratios (ω) for seven different branch categories: Mysticeti, Odontoceti, Functional, a
189 category corresponding to the common cetacean branch, other concerning the stem Mysticeti
190 branch, an additional one regarding the stem Odontoceti branch (excluding *Physeter catodon*, the
191 sperm whale) and finally, a category corresponding to the *Physeter catodon* (sperm whale)
192 ancestor branch. Mysticeti and Odontoceti branch categories comprised all predicted Mysticeti
193 and Odontoceti DRD₅ sequences, respectively. The Functional branch category comprised
194 *Hippopotamus amphibius* (hippopotamus), *Bos taurus* (cattle) and *Homo sapiens* (human) DRD₅

195 coding sequences. For each of the seven different branch categories, likelihood ratio tests (LRT)
196 (following χ^2 distribution) were conducted to compare the estimated ratio (ω) of the
197 nonsynonymous substitution rate (dN) to the synonymous substitution rate (dS) determined by
198 PAML (the alternative hypothesis), with the expected ratio (ω) of the nonsynonymous
199 substitution rate (dN) to the synonymous substitution rate (dS) according to a neutral model of
200 evolution ($\omega = 1$) (the null hypothesis). All PAML analyses were run with the CodonFreq set to 3
201 and codon sites with ambiguous data (including gaps and missing data) were included in the
202 analyses.

203

204 **Results**

205 To examine the annotation tags and distribution of the DRD₅ gene across mammals, 119
206 annotated mammalian genomes available at NCBI were scrutinized for the presence of DRD₅
207 gene annotation and each respective protein product description screened for the ‘low-quality
208 protein’ (LQ) tag. This examination resulted in 10 species presenting the DRD₅ LQ tag,
209 including *Ovis aries* (sheep), *Phascolarctos cinereus* (koala), *Bison bison bison* (plains bison),
210 *Myotis davidii* (vesper bat), *Ochotona princeps* (American pika) and 5 cetacean species. The
211 latter included *Lagenorhynchus obliquidens* (Pacific white-sided dolphin), *N. a. asiaorientalis*
212 (Yangtze finless porpoise), *D. leucas* (beluga whale), *Physeter catodon* (sperm whale) and
213 *Orcinus orca* (killer whale). Each genomic sequence corresponding to the DRD₅ LQ annotations
214 was examined and the coding sequence (CDS) manually predicted (Lopes-Marques et al., 2017).
215 Given the prominence of DRD₅ LQ annotations in Cetacea we scrutinized other cetacean species
216 with available, but unannotated genomes, *Balaenoptera bonaerensis* (Antarctic minke whale),
217 *Eschrichtius robustus* (gray whale), *Balaena mysticetus* (bowhead whale), *S. chinensis* (Indo-
218 Pacific humpback dolphin), or with annotated genomes lacking DRD₅ annotations: *Lipotes*
219 *vexillifer* (Yangtze River dolphin) and *Balaenoptera acutorostrata scammoni* (minke whale)
220 (Supplementary Figure 1). Additionally, *T. truncatus* (bottlenose dolphin), presenting a
221 seemingly intact DRD₅ gene annotation, without the ‘low-quality protein’ tag (LQ), as well as
222 *Hippopotamus amphibius* (common hippopotamus) predicted DRD₅ coding sequence,
223 representing the closest extant lineage of Cetacea, were equally inspected. Other mammals with
224 annotated genome without DRD₅ gene annotation were also scrutinised, namely: *Microcebus*

225 *murinus* (gray mouse lemur), *Jaculus jaculus* (lesser Egyptian jerboa), *Chrysochloris asiatica*
226 (Cape golden mole), *Erinaceus europaeus* (western European hedgehog), *Elephantulus edwardii*
227 (Cape elephant shrew) and *Condylura cristata* (star-nosed mole). In total, 124 mammalian
228 species were inspected and an in-depth description regarding analysed species list and genomic
229 sequences accession numbers are available at Supplementary Table 2. The Supplementary Figure
230 2 presents a multiple translation alignment of the NCBI non-LQ tagged mammalian DRD₅
231 orthologous sequences. The alignment also includes the predicted *Hippopotamus amphibius*
232 (hippopotamus) DRD₅ sequence and excludes *T. truncatus* (common bottlenose dolphin) DRD₅
233 sequence, afterwards demonstrated to contain inactivating mutations (see below). The examined
234 sequences exhibit a substantial degree of conservation (average pairwise identity of over 80%),
235 with minor variation in the expected protein size. The protein sequence conservation is
236 particularly noticeable at the c-terminus (Supplementary Figure 2).

237

238 **ORF disrupting mutations of DRD₅ in Cetacea**

239 For cetacean species with annotated genomes, we started by examining the DRD₅ gene
240 locus, including neighbouring genes, to verify and elucidate the orthology of the annotated and
241 non-annotated genes and outline the genomic regions to be inspected (Supplementary Figure 1).
242 All analysed loci were found to be conserved, including in both *Lipotes vexillifer* (Yangtze River
243 dolphin) and *Balaenoptera acutorostrata scammoni* (minke whale), which lacked previous
244 DRD₅ gene annotations (Supplementary figure 1). Subsequent manual annotation of all collected
245 cetacean genomic sequences revealed DRD₅ gene erosion across all analysed species, except in
246 *Balaenoptera acutorostrata scammoni* (minke whale), for which the DRD₅ coding status could
247 not be accessed due to fragmentation of the 5' end of the respective genomic region (presence of
248 sequencing gaps (Ns)). In detail, a conserved 2 nucleotide deletion was detected for the full set of
249 Odontoceti examined species, except for *Physeter catodon* (sperm whale) that presented a
250 premature stop codon near the middle of the gene and a single nucleotide insertion close to the
251 end of the gene (Figure 1). The 2-nucleotide deletion alters the reading frame, leading to a drastic
252 change in downstream amino acid composition. Additionally, non-conserved mutations were
253 found in *Lipotes vexillifer* (Yangtze River dolphin), which presented 2 premature stop codons, *N.*
254 *a. asiaeorientalis* (Yangtze finless porpoise) that presented a premature stop codon close to the
255 middle of the ORF, and *D. leucas* (beluga whale) with a single nucleotide deletion near the 5'

256 end of the gene (Figure 1). *D. leucas* (beluga whale) presumed DRD₅ sequence presented another
257 noticeable feature. A massive and abrupt alignment identity decrease observed when aligning
258 *Bos taurus* (cattle) DRD₅ gene against the genomic target region of *D. leucas* (beluga whale).
259 The alignment identity drop was noted approximately in the middle of the complete alignment
260 length for this species, suggesting that the DRD₅ gene sequence is interrupted, and further
261 supporting pseudogenization in this species. Regarding Odontoceti, at least one ORF-abolishing
262 mutation was validated using available genomic Sequence Read Archives (SRAs) experiments
263 for all studied species, excluding *S. chinensis* (Indo-pacific humpbacked dolphin) and *Lipotes*
264 *vexillifer* (Yangtze River dolphin) for which no genomic sequencing runs were available at the
265 NCBI SRA database (Supplementary Material 1).

266 Regarding the Mysticeti suborder, a conserved single nucleotide deletion was detected in all
267 species except *Balaenoptera acutorostrata scammoni* (minke whale) (Figure 1). A non-
268 conserved 2 nucleotide insertion was found also found in *Balaenoptera bonaerensis* (Antartic
269 minke whale) and an insertion of one nucleotide was detected at *Eschrichtius robustus* (grey
270 whale) near the 5' end of the DRD₅ sequence (Figure 1). Again, at least one ORF-abolishing
271 mutation was validated using genomic SRA experiments for all analysed species (Supplementary
272 Material 1). Importantly, no conserved mutations were detected between most Odontoceti,
273 *Physeter catodon* (sperm whale, Odontoceti) and Mysticeti lineages, suggesting that DRD₅ three
274 pseudogenization events occurred independently after their evolutionary divergence (Figure 1).
275 To increase the robustness of our analysis, we further scrutinized the genome of the extant sister
276 clade of the Cetacea, the Hippopotamidae and were able to predict a fully coding sequence for
277 DRD₅ in *Hippopotamus amphibius* (hippopotamus), supporting the loss of DRD₅ after Cetacea
278 diversification.

279

280 **dN/dS analyses support independent inactivation events of DRD₅ in Cetacea lineages**

281 To further strengthen the mutational analyses, we next carried out a dN/dS approach. The
282 dN/dS analyses for species with functional DRD₅ gene (Functional branches category) rejected
283 the null hypothesis ($\omega = 1$, $p = 0.0300$, $< .05$), confirming that, as expected, these have evolved
284 under purifying selection ($\omega < 1$), favoring the conservation of DRD₅ in the tested lineages
285 (Table 1). In contrast, concerning Mysticeti and Odontoceti branch categories, the performed
286 analyses failed to reject the null hypothesis ($p = 0.692$ for Odontoceti branches category and $p =$

287 0.291 for Mysticeti branches category respectively) suggesting that DRD₅ evolved neutrally in
288 both lineages, following a gene inactivation event (Table 1). Moreover, evidences of purifying
289 selection were found for the common Cetacean branch category ($\omega = 0.135$, $p = 0.001$),
290 suggesting the existence of a functional DRD₅ in the common ancestral to all cetaceans (Table
291 1). Purifying selection was also detected for the Odontoceti stem branch category (excluding
292 *Physeter catodon*, the sperm whale) ($\omega = 0.213$, $p = 0.045$). In contrast the *Physeter catodon*
293 (sperm whale) ancestor branch category, does not present a dN/dS ratio (ω) statistically
294 significantly different from 1 ($\omega = 0.320$, $p = 0.460$) (Table 1). Together with the mutational
295 evidences (Figure 1), these results suggest two independent inactivation events within the
296 Odontoceti. Regarding the Mysticeti stem branch category, selection analysis showed evidence
297 of neutral selection ($\omega = 1.174$, $p = 0.905$) (Table 1). However, mutational evidence supports a
298 conserved inactivation event in the common ancestor of Mysticeti. Taken together, our results
299 support three independent DRD₅ inactivation events in Cetacea.

300

301 **Other mammalian species displaying DRD₅ LQ tags have a coding gene**

302 Initial analysis revealed the presence of at least one ORF-abolishing mutation in *Ovis aries*
303 (sheep), *Phascolarctos cinereus* (koala), *Bison bison bison* (plains bison) and *Ochotona princeps*
304 (American pika). These are in some cases suggestive of gene inactivation and not sequencing
305 artefacts (e.g. Emerling et al., 2017; Lopes-Marques et al., 2017). Manual annotation, including
306 SRA validation, unveiled sequencing reads supporting the absence of disruptive ORF mutations,
307 rebutting each inactivation mutation and suggesting that DRD₅ is, in fact, coding in these species
308 (Supplementary Material 2). Regarding *Myotis davidii* (vesper bat), the fragmentation of the
309 genomic region (Ns) flanked by upstream and downstream DRD₅ neighbouring genes impeded
310 us to infer the DRD₅ coding status in this species. Interestingly, regarding *Ochotona princeps*
311 (American pika) mutational SRA validation, two scenarios were observed: approximately 50%
312 of aligned reads supported the presence of a premature stop codon in the DRD₅ gene of this
313 species, with the remaining set of aligning reads supporting the absence of a premature stop
314 codon in the same species. This suggest that an allelic pseudogenization event might have
315 occurred in this species.

316

317

318 ***Chrysochloris asiatica* presents a non-functional DRD₅ gene**

319 Next, we examined other mammalian species with annotated genome yet lacking DRD₅ gene
320 annotations. Results were inconclusive regarding the coding status of *Microcebus murinus* (gray
321 mouse lemur), *Condylura cristata* (star-nosed mole), *J. jaculus* (lesser Egyptian jerboa) and
322 *Erinaceus europaeus* (western European hedgehog) DRD₅, due to the fragmentation (Ns) of the
323 genomic region flanked by the upstream and downstream DRD₅ neighbouring genes, and the
324 unavailability of whole genome shotgun contigs spanning our target gene. For *Elephantulus*
325 *edwardii* (Cape elephant shrew) we were able to deduce a fully DRD₅ coding sequence. Curiously,
326 *Chrysochloris asiatica* (Cape golden mole) presented a single nucleotide insertion in the 5' end of
327 the gene (validated by genomic SRA, see Supplementary Material 3), suggesting that DRD₅ might
328 be pseudogenized in this species.

329

330 **Discussion**

331 The rise of large-scale genomic sequencing projects has emphasized the role of gene loss as
332 a potent driver of evolutionary change: underlying phenotypic adaptations or neutral regressions
333 in response to specific environmental cues and niches (Albalat & Canestro, 2016; Braun, 2003;
334 Jebb & Hiller, 2018; Jeffery, 2009; Olson, 1999; Sadier et al., 2018; Sharma et al., 2018;
335 Somorjai et al., 2018). By comparing 124 mammalian genomes, we document three independent
336 erosion events of a dopamine receptor, DRD₅, in Cetacea lineages. Although the current analysis
337 is highly dependent of the quality of genome sequencing projects and their assembly, the
338 conserved mutational profile of DRD₅ gene inactivation within Cetacea lineages further
339 strengthens our findings.

340 Dopamine, a neurotransmitter and signalling molecule, is involved in distinct functions both
341 in the central nervous system and peripheral tissues: including movement, feeding, sleep, reward,
342 learning and memory as well as in the regulation of olfaction, hormone pathways, renal
343 functions, immunity, sympathetic regulation and cardiovascular functions, respectively (Beaulieu
344 & Gainetdinov, 2011). More specifically, the disruption of DRD₅-dependent pathways in rodents
345 was shown to increase blood pressure and sympathetic tone, promoting vasoconstriction, thus
346 yielding a hypertensive phenotype (Hollon et al., 2002; Li et al., 2008).

347 The observed gene loss distribution, and predicted phenotypic outcome, is consistent with
348 the peripheral vasoconstriction mechanism described in Cetacea, suggested to counterbalance

349 deep-diving induced hypoxia (Ramirez et al., 2007; Tian et al., 2016). In fact, Cetacea have
350 developed a number of physiological adaptations to offset hypoxia: notably, increased blood
351 volume and oxygen-transport protein levels (hemoglobin, neuroglobin and myoglobin), allowing
352 oxygen stores in blood, muscle tissues, and brain, reduced heart rate or bradycardia, apnea and
353 peripheral vasoconstriction (Nery et al., 2013; Panneton, 2013; Ramirez et al., 2007; Tian et al.,
354 2016). Peripheral vasoconstriction allows the regional compartmentalization of blood supplies,
355 reducing blood flow in more hypoxia-tolerant tissues, such as skin, muscle, spleen or kidney,
356 while maintaining arterial blood flow to the central nervous system and heart (Panneton, 2013).
357 Moreover, the deviation of muscle blood supply reduces lactate accumulation (Panneton, 2013).
358 Thus, in Cetacea, DRD₅ loss could contribute for the peripheral vasoconstriction requirements of
359 diving. Also, by shifting renal salt balance, DRD₅ could also play a role in the maintenance of an
360 adequate blood volume and pressure (Bie, 2009; Hong et al., 2017; Li et al., 2008; Zeng et al.,
361 2005).

362 The predicted vasoconstriction phenotype is in agreement with a previous work reporting
363 episodes of adaptive evolution (positive selection) in genes related with hypoxia tolerance in
364 Cetacea, including genes involved in oxygen transport and regulation of vasoconstriction (Tian
365 et al., 2016). In addition, by expanding their analysis to other non-aquatic hypoxic environments,
366 such as underground tunnels, they uncovered convergent evolution scenarios in species adapted
367 to diving and burrowing (Tian et al., 2016). A similar convergence is observed in the present
368 work. In fact, in the mole *Chrysochloris asiatica* (Cape golden mole), DRD₅ was also predicted
369 non-functional. Although this was the single DRD₅ loss example found outside Cetacea, one
370 cannot discard the putative contribution of alternative molecular events (i.e. post-translational
371 mechanisms) towards trait loss (Sadier et al., 2018), or event distinct physiological adaptations to
372 overcome oxygen deprivation.

373 Besides diving physiology, DRD₅-dependent sympathetic tone alterations could also
374 contribute to the idiosyncratic sleep behavior observed in Cetacea (Huelsmann et al., 2019;
375 Lopes-Marques et al., 2019b; Lyamin et al., 2008). Several physiological adjustments occur
376 during sleep, encompassing thermoregulation, as well as endocrine, immune, pulmonary and
377 cardiovascular functions (Giglio et al., 2007). In most mammals, sleep states lead to a decrease
378 of the sympathetic tone, inducing vasodilation and decreasing blood pressure (Giglio et al.,

379 2007). Thus, DRD₅ loss could prevent sympathetic tone decrease in resting states paralleling the
380 unihemispheric sleeping behavior and long-term vigilance observed in Cetacea.

381

382 **Conclusions**

383 Overall, our findings provide evidence for natural occurring KO for DRD₅. Besides highlighting
384 a molecular signature for vasoconstriction and blood pressure regulation in Cetacea, naturally
385 occurring DRD₅ KO could also provide useful frameworks to gain insight into hypertension and
386 heart failure-induced peripheral vasoconstriction responses in humans (Triposkiadis et al., 2009;
387 Wang et al., 2008).

388

389 **Acknowledgements**

390 We acknowledge the various genome consortiums for sequencing and assembling the genomes.

391

392

393 **References**

- 394 Albalat R, Canestro C. 2016. Evolution by gene loss. *Nature Reviews Genetics* 17:379-391. 10.1038/nrg.2016.39
- 395 Ariano MA, Wang J, Noblett KL, Larson ER, Sibley DR. 1997. Cellular distribution of the rat D1B receptor in central
396 nervous system using anti-receptor antisera. *Brain Research* 746:141-150. [https://doi.org/10.1016/S0006-
397 8993\(96\)01219-X](https://doi.org/10.1016/S0006-8993(96)01219-X)
- 398 Beaulieu J-M, Gainetdinov RR. 2011. The Physiology, Signaling, and Pharmacology of Dopamine Receptors.
399 *Pharmacological Reviews* 63:182. 10.1124/pr.110.002642
- 400 Bie P. 2009. Blood volume, blood pressure and total body sodium: internal signalling and output control. *Acta*
401 *Physiologica* 195:187-196. 10.1111/j.1748-1716.2008.01932.x
- 402 Braun EL. 2003. Innovation from reduction: gene loss, domain loss and sequence divergence in genome evolution.
403 *Applied Bioinformatics* 2:13-34.
- 404 Ciliax BJ, Nash N, Heilman C, Sunahara R, Hartney A, Tiberi M, Rye DB, Caron MG, Niznik HB, Levey AI. 2000.
405 Dopamine D5 receptor immunolocalization in rat and monkey brain. *Synapse* 37:125-145. 10.1002/1098-
406 2396(200008)37:2<125::AID-SYN7>3.0.CO;2-7
- 407 Dahmer MK, Senogles SE. 1996. Dopaminergic Inhibition of Catecholamine Secretion from Chromaffin Cells: Evidence
408 that Inhibition Is Mediated by D4 and D5 Dopamine Receptors. *Journal of Neurochemistry* 66:222-232.
409 10.1046/j.1471-4159.1996.66010222.x
- 410 Daly G, Hawi Z, Fitzgerald M, Gill M. 1999. Mapping susceptibility loci in attention deficit hyperactivity disorder:
411 preferential transmission of parental alleles at DAT1, DBH and DRD5 to affected children. *Molecular Psychiatry*
412 4:192. 10.1038/sj.mp.4000510
- 413 Emerling CA, Widjaja AD, Nguyen NN, Springer MS. 2017. Their loss is our gain: regressive evolution in vertebrates
414 provides genomic models for uncovering human disease loci. *Journal of Medical Genetics* 54:787.
415 10.1136/jmedgenet-2017-104837
- 416 Giglio P, Lane JT, Barkoukis TJ, Dumitru I. 2007. Sleep Physiology. In: Barkoukis TJ, and Avidan AY, eds. *Review of*
417 *Sleep Medicine (Second Edition)*. Philadelphia: Butterworth-Heinemann, 29-41.
- 418 Guindon S, Dufayard J-F, Lefort V, Anisimova M, Hordijk W, Gascuel O. 2010. New Algorithms and Methods to
419 Estimate Maximum-Likelihood Phylogenies: Assessing the Performance of PhyML 3.0. *Systematic Biology*
420 59:307-321. 10.1093/sysbio/syq010
- 421 Hollon TR, Bek MJ, Lachowicz JE, Ariano MA, Mezey E, Ramachandran R, Wersinger SR, Soares-da-Silva P, Liu ZF,
422 Grinberg A, Drago J, Young WS, Westphal H, Jose PA, Sibley DR. 2002. Mice Lacking D5 Dopamine Receptors

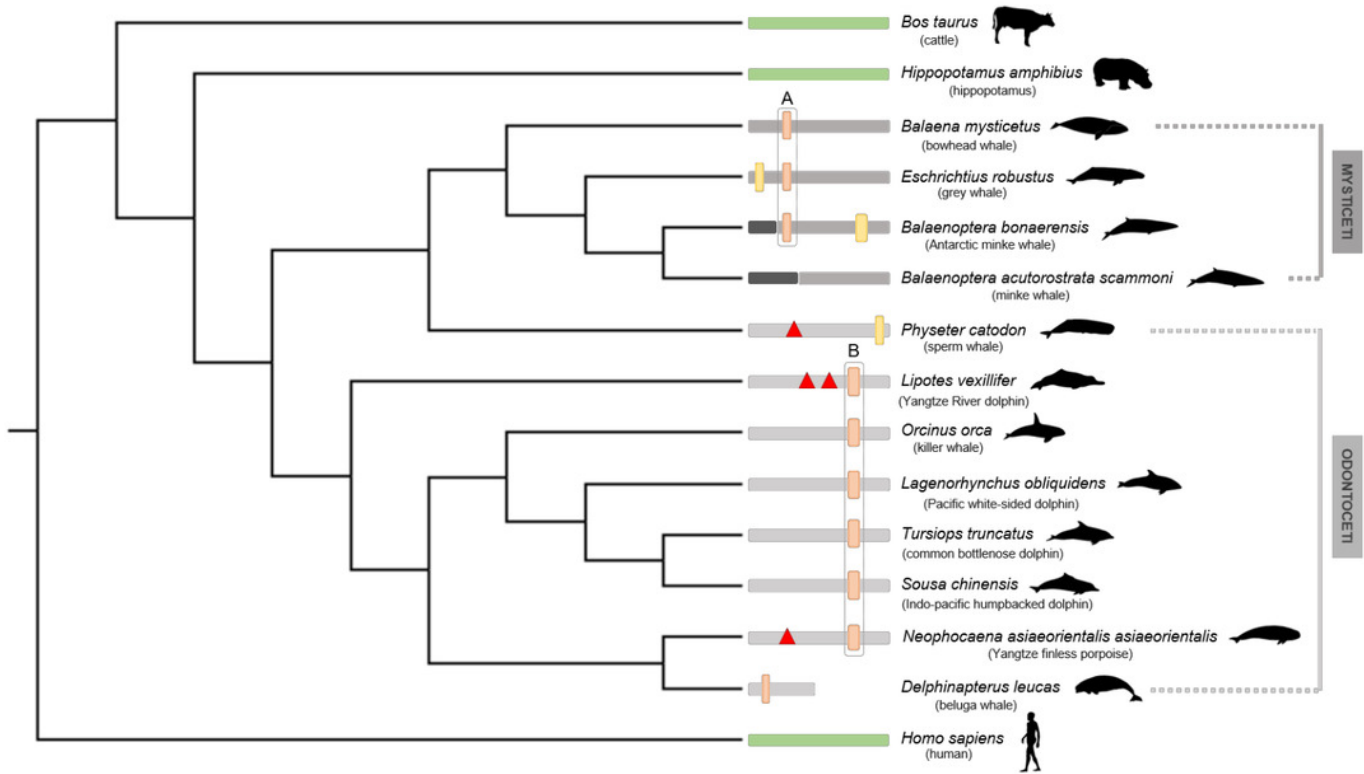
- 423 Have Increased Sympathetic Tone and Are Hypertensive. *The Journal of Neuroscience* 22:10801.
424 10.1523/JNEUROSCI.22-24-10801.2002
- 425 Hong K, Li M, Nourian Z, Meiningner GA, Hill MA. 2017. Angiotensin II Type 1 Receptor Mechanoactivation Involves
426 RGS5 (Regulator of G Protein Signaling 5) in Skeletal Muscle Arteries: Impaired Trafficking of RGS5 in
427 Hypertension. *Hypertension (Dallas, Tex : 1979)* 70:1264-1272. 10.1161/HYPERTENSIONAHA.117.09757
- 428 Huelsmann M, Hecker N, Springer MS, Gatesy J, Sharma V, Hiller M. 2019. Genes lost during the transition from land
429 to water in cetaceans highlight genomic changes involved in aquatic adaptations. *bioRxiv*. 10.1101/521617
- 430 Jebb D, Hiller M. 2018. Recurrent loss of HMGC2 shows that ketogenesis is not essential for the evolution of large
431 mammalian brains. *eLife* 7. 10.7554/eLife.38906
- 432 Jeffery WR. 2009. Regressive evolution in *Astyanax* cavefish. *Annual Review of Genetics* 43:25-47. 10.1146/annurev-genet-
433 102108-134216
- 434 Kumar S, Dudley JT, Filipinski A, Liu L. 2011. Phylomedicine: an evolutionary telescope to explore and diagnose the
435 universe of disease mutations. *Trends in Genetics* 27:377-386. 10.1016/j.tig.2011.06.004
- 436 Lachner J, Mlitz V, Tschachler E, Eckhart L. 2017. Epidermal cornification is preceded by the expression of a
437 keratinocyte-specific set of pyroptosis-related genes. *Scientific Reports* 7:17446. 10.1038/s41598-017-17782-4
- 438 Lefort V, Longueville J-E, Gascuel O. 2017. SMS: Smart Model Selection in PhyML. *Molecular Biology and Evolution*
439 34:2422-2424. 10.1093/molbev/msx149
- 440 Li H, Armando I, Yu P, Escano C, Mueller SC, Asico L, Pascua A, Lu Q, Wang X, Villar VAM, Jones JE, Wang Z,
441 Periasamy A, Lau Y-S, Soares-da-Silva P, Creswell K, Guillemette G, Sibley DR, Eisner G, Felder RA, Jose PA.
442 2008. Dopamine 5 receptor mediates Ang II type 1 receptor degradation via a ubiquitin-proteasome pathway
443 in mice and human cells. *The Journal of Clinical Investigation* 118:2180-2189. 10.1172/JCI33637
- 444 Lopes-Marques M, Machado AM, Alves QL, Fonseca MM, Barbosa S, Sinding M-HS, Rasmussen MH, Iversen MR,
445 Bertelsen MF, Campos PF, da Fonseca R, Ruivo R, Castro LFC. 2019a. Complete inactivation of sebum-
446 producing genes parallels the loss of sebaceous glands in Cetacea (in press). *Molecular Biology and Evolution*.
- 447 Lopes-Marques M, Machado AM, Barbosa S, Fonseca MM, Ruivo R, Castro LFC. 2018. Cetacea are natural knockouts
448 for IL20. *Immunogenetics*. 10.1007/s00251-018-1071-5
- 449 Lopes-Marques M, Ruivo R, Alves QL, Sousa N, Machado MA, Castro FL. 2019b. The Singularity of Cetacea Behavior
450 Parallels the Complete Inactivation of Melatonin Gene Modules. *Genes* 10. 10.3390/genes10020121
- 451 Lopes-Marques M, Ruivo R, Fonseca E, Teixeira A, Castro LFC. 2017. Unusual loss of chymosin in mammalian lineages
452 parallels neo-natal immune transfer strategies. *Molecular Phylogenetics and Evolution* 116:78-86.
453 <https://doi.org/10.1016/j.ympev.2017.08.014>
- 454 Lyamin OI, Manger PR, Ridgway SH, Mukhametov LM, Siegel JM. 2008. Cetacean sleep: An unusual form of
455 mammalian sleep. *Neuroscience & Biobehavioral Reviews* 32:1451-1484. 10.1016/j.neubiorev.2008.05.023
- 456 McGowen MR, Gatesy J, Wildman DE. 2014. Molecular evolution tracks macroevolutionary transitions in Cetacea.
457 *Trends in Ecology & Evolution* 29:336-346. <https://doi.org/10.1016/j.tree.2014.04.001>
- 458 Mezey E, Eisenhofer G, Harta G, Hansson S, Gould L, Hunyady B, Hoffman BJ. 1996. A novel nonneuronal
459 catecholaminergic system: exocrine pancreas synthesizes and releases dopamine. *Proceedings of the National
460 Academy of Sciences* 93:10377. 10.1073/pnas.93.19.10377
- 461 Miller MP, Kumar S. 2001. Understanding human disease mutations through the use of interspecific genetic variation.
462 *Human Molecular Genetics* 10:2319-2328. 10.1093/hmg/10.21.2319
- 463 Muir WJ, Thomson ML, McKeon P, Mynett-Johnson L, Whitton C, Evans KL, Porteous DJ, Blackwood DHR. 2001.
464 Markers close to the dopamine D5 receptor gene (DRD5) show significant association with schizophrenia but
465 not bipolar disorder. *American Journal of Medical Genetics* 105:152-158. 10.1002/1096-
466 8628(2001)9999:9999<:AID-AJMG1163>3.0.CO;2-2
- 467 Nery MF, Arroyo JI, Opazo JC. 2013. Accelerated Evolutionary Rate of the Myoglobin Gene in Long-Diving Whales.
468 *Journal of Molecular Evolution* 76:380-387. 10.1007/s00239-013-9572-1
- 469 Nery MF, Arroyo JI, Opazo JC. 2014. Increased rate of hair keratin gene loss in the cetacean lineage. *BMC Genomics*
470 15:869. 10.1186/1471-2164-15-869
- 471 Olson MV. 1999. When less is more: gene loss as an engine of evolutionary change. *American Journal of Human Genetics*
472 64:18-23. 10.1086/302219
- 473 Opazo JC, Zavala K, Miranda-Rottmann S, Araya R. 2018. Evolution of dopamine receptors: phylogenetic evidence
474 suggests a later origin of the DRD2l and DRD4rs dopamine receptor gene lineages. *PeerJ* 6:e4593.
475 10.7717/peerj.4593

- 476 Ott T, Nieder A. 2018. Dopamine and Cognitive Control in Prefrontal Cortex. *Trends in Cognitive Sciences*.
477 10.1016/j.tics.2018.12.006
- 478 Panneton WM. 2013. The mammalian diving response: an enigmatic reflex to preserve life? *Physiology (Bethesda, Md)*
479 28:284-297. 10.1152/physiol.00020.2013
- 480 Rambaut A, Drummond AJ. 2012. FigTree version 1.4.0.
- 481 Ramirez J-M, Folkow LP, Blix AS. 2007. Hypoxia Tolerance in Mammals and Birds: From the Wilderness to the Clinic.
482 *Annual Review of Physiology* 69:113-143. 10.1146/annurev.physiol.69.031905.163111
- 483 Sadier A, Davies KTJ, Yohe LR, Yun K, Donat P, Hedrick BP, Dumont ER, Dávalos LM, Rossiter SJ, Sears KE. 2018.
484 Multifactorial processes underlie parallel opsin loss in neotropical bats. *eLife* 7:e37412. 10.7554/eLife.37412
- 485 Sanada H, Xu J, Jose PA, Watanabe H, Felder RA. 2000. Differential expression and regulation of dopamine-1(d1) and
486 dopamine-5(d-5) receptor function in human kidney. *American Journal of Hypertension* 13:156A-156A.
487 10.1016/S0895-7061(00)00649-X
- 488 Sharma V, Hecker N, Roscito JG, Foerster L, Langer BE, Hiller M. 2018. A genomics approach reveals insights into the
489 importance of gene losses for mammalian adaptations. *Nature Communications* 9:1215. 10.1038/s41467-018-
490 03667-1
- 491 Somorjai IML, Martí-Solans J, Diaz-Gracia M, Nishida H, Imai KS, Escrivà H, Cañestro C, Albalat R. 2018. Wnt
492 evolution and function shuffling in liberal and conservative chordate genomes. *Genome Biology* 19:98.
493 10.1186/s13059-018-1468-3
- 494 Springer MS, Murphy WJ. 2007. Mammalian evolution and biomedicine: new views from phylogeny. *Biological Reviews*
495 82:375-392. 10.1111/j.1469-185X.2007.00016.x
- 496 Strasser B, Mlitz V, Fischer H, Tschachler E, Eckhart L. 2015. Comparative genomics reveals conservation of filaggrin
497 and loss of caspase-14 in dolphins. *Exp Dermatol* 24:365-369. 10.1111/exd.12681
- 498 Sunahara RK, Guan H-C, O'Dowd BF, Seeman P, Laurier LG, Ng G, George SR, Torchia J, Van Tol HHM, Niznik HB.
499 1991. Cloning of the gene for a human dopamine D5 receptor with higher affinity for dopamine than D1.
500 *Nature* 350:614-619. 10.1038/350614a0
- 501 Tian R, Wang Z, Niu X, Zhou K, Xu S, Yang G. 2016. Evolutionary Genetics of Hypoxia Tolerance in Cetaceans during
502 Diving. *Genome biology and evolution* 8:827-839. 10.1093/gbe/evw037
- 503 Tiberi M, Caron MG. 1994. High agonist-independent activity is a distinguishing feature of the dopamine D1B receptor
504 subtype. *Journal of Biological Chemistry* 269:27925-27931.
- 505 Triposkiadis F, Karayannis G, Giamouzis G, Skoularigis J, Louridas G, Butler J. 2009. The Sympathetic Nervous System
506 in Heart Failure: Physiology, Pathophysiology, and Clinical Implications. *Journal of the American College of*
507 *Cardiology* 54:1747-1762. <https://doi.org/10.1016/j.jacc.2009.05.015>
- 508 Vanyukov MM, Moss HB, Gioio AE, Hughes HB, Kaplan BB, Tarter RE. 1998. An Association Between a Microsatellite
509 Polymorphism at the DRD5 Gene and the Liability to Substance Abuse: Pilot Study. *Behavior Genetics* 28:75-
510 82. 10.1023/A:1021463722326
- 511 Wang X, Villar VAM, Armando I, Eisner GM, Felder RA, Jose PA. 2008. Dopamine, kidney, and hypertension: studies
512 in dopamine receptor knockout mice. *Pediatric nephrology (Berlin, Germany)* 23:2131-2146. 10.1007/s00467-008-
513 0901-3
- 514 Yang Z. 2007. PAML 4: Phylogenetic Analysis by Maximum Likelihood. *Molecular Biology and Evolution* 24:1586-1591.
515 10.1093/molbev/msm088
- 516 Zeng C, Yang Z, Wang Z, Jones J, Wang X, Altea J, Mangrum Amy J, Hopfer U, Sibley David R, Eisner Gilbert M, Felder
517 Robin A, Jose Pedro A. 2005. Interaction of Angiotensin II Type 1 and D5 Dopamine Receptors in Renal
518 Proximal Tubule Cells. *Hypertension* 45:804-810. 10.1161/01.HYP.0000155212.33212.99
- 519

Figure 1

Schematic representation of the DRD5 gene ORF abolishing annotated mutations regarding Cetacea parvorders Odontoceti and Mysticeti.

Phylogenetic relationships derived from a Maximum Likelihood (ML) tree with the DRD5 sequences from Mysticeti and Odontoceti species, as well as from *Hippopotamus amphibius* (hippopotamus), *Bos taurus* (cattle) and *Homo sapiens* (human). DRD₅ ORF-abolishing mutations are mapped in the corresponding branch. Vertical thick bars represent 2-nucleotide insertions (yellow) or deletions (orange). Vertical thin bars represent single nucleotide insertion (yellow) or deletion (orange). In-frame premature stop codons are represented by red triangles. Fragmented or incomplete genomic regions are represented by black regions. *Delphinapterus leucas* (beluga whale) predicted DRD₅ shortness is represented by a smaller bar. Functional branches are represented by green bars, nonfunctional branches are represented by grey and dark grey bars (Odontoceti and Mysticeti branches, respectively). Example of DRD₅ open reading frame (ORF) inactivating mutations concerning Mysticeti clade (A) and Odontoceti clade (excluding *Physeter catodon*, the sperm whale) (B). Numbers above characters represent the alignment position index.



A

	642	654
	
<i>Bos taurus</i>	AACTGCGACTCCA	
<i>Balaena mysticetus</i>	AACTGTGA-TCCA	
<i>Eschrichtius robustus</i>	AACTGTGA-TCCA	
<i>Balaenoptera bonaerensis</i>	AACTGTGA-TCCA	

B

	1251	1262
	
<i>Bos taurus</i>	GACAAGGAGGAG	
<i>Lipotes vexillifer</i>	GACAA--AGGAG	
<i>Orcinus orca</i>	GACAA--AGGAG	
<i>Lagenorhynchus obliquidens</i>	GACAA--AGGAG	
<i>Tursiops truncatus</i>	GACAA--AGGAG	
<i>Sousa chinensis</i>	GACAA--AGGAG	
<i>Neophocaena asiaeorientalis asiaeorientalis</i>	GACAA--AGGAG	

Legend:

- █ 1-nucleotide insertion
- █ 2-nucleotide insertion
- █ 1-nucleotide deletion
- █ 2-nucleotide deletion
- ▲ Premature stop codon
- Fragmented/incomplete genomic region
- Functional gene

Table 1 (on next page)

Selection (dN/dS) analyses with CODEML from PAML for the seven different branch categories.

Likelihood ratio tests (LRT) corresponding p -value concerning each branch category is also presented.

1

2 **Table 1:** Results of selection (dN/dS) analyses with CODEML from PAML for the seven
 3 different branch categories. Likelihood ratio tests (LRT) corresponding p -value concerning each
 4 branch category is also presented.

Branch category	dN/dS (ω)
Functional branches (<i>Homo sapiens</i> , <i>Bos taurus</i> , <i>Hippopotamus amphibius</i>)	Statistically significantly \neq from 1 ($p = 0.0300$)
Mysticeti branches (<i>Balaena mysticetus</i> , <i>Eschrichtius robustus</i> , <i>Balaenoptera bonaerensis</i> , <i>Balaenoptera acutorostrata scammoni</i>)	Not statistically significantly \neq from 1 ($p = 0.291$)
Odontoceti branches (<i>Physeter catodon</i> , <i>Lipotes vexillifer</i> , <i>Orcinus orca</i> , <i>Lagenorhynchus obliquidens</i> , <i>Tursiops truncatus</i> , <i>Sousa chinensis</i> , <i>Neophocanea asiaeorientalis asiaeorientalis</i>)	Not statistically significantly \neq from 1 ($p = 0.692$)
Common cetacean branch	0,135 ($p = 0.001$, statistically significantly \neq from 1)
Stem Mysticeti branch	1.174 ($p = 0.905$, not statistically significantly \neq from 1)
Stem Odontoceti (excluding <i>Physeter catodon</i>, sperm whale) branch	0.213 ($p = 0.045$, statistically significantly \neq from 1)
<i>Physeter catodon</i> (sperm whale) ancestor branch	0.320, ($p = 0.460$, not statistically significantly \neq from 1)

5

6